Available online at www.sciencedirect.com
SCIENCE DIRECT®
Chemical Physics Letters 414 (2005) 155–160
CHEMICAL PHYSICS LETTERS
www.elsevier.com/locate/cplett

Molecular dynamics study of photochromic molecules probed by the mask pattern transferred transient grating technique

Koichi Okamoto [a,*], Terrell D. Neal [a], Zhaoyu Zhang [a], David T. Wei [b], Axel Scherer [a]

[a] *Department of Electrical Engineering and Physics, California Institute of Technology, Caltech Mail Code 136-93, 1200 E. California Blvd. Pasadena, CA 91125, United States*
[b] *Wei and Associates, 3715 Malibu Vista Dr, Malibu, CA 90265, United States*

Received 6 July 2005; in final form 4 August 2005
Available online 2 September 2005

Abstract

Mask pattern transferred transient grating, which is a convenient new technique in the class of optical heterodyne detected transient grating, is applied to photochromic molecule (spiropyran) in 2-propanol solution. The spatial modulations of optical properties of the material is generated by transferring an ultra-violet light pattern directly from a metal film grating into the sample solution and detected through the diffraction of a probe beam. The thermal conductivity of the solvent and the diffusion coefficients of the solute molecules were obtained and compared with the calculated values. This method has many advantages compared to the conventional techniques.

1. Introduction

The transient grating (TG) technique, which is one of the third order nonlinear spectroscopies, has been a useful and powerful tool for studies in photonics and in photochemical processes of solutions [1–6]. This technique has many unique advantages. For example, this technique is capable of monitoring molecular dynamics of short lived chemical species in solutions [7–10]. However, there are several difficulties in this technique. The diffracted signal intensity (I_{TG}) is given by the sum of the square of refractive index change (δn; phase grating) and absorbance change (δk; amplitude grating) induced by the optical interference pattern. Quadratic nature of the signal intensity makes the analysis of the signal components complicated. Also, contributions of the phase and amplitude gratings are difficult to separate from each other. Another difficulty of this technique is its weak signal intensities, so that a highly sensitive optical detection technique has been required.

In order to improve these difficulties, the optical heterodyne detected transient grating (OHD-TG) has been devised [11,12]. In this technique, a local oscillator field is mixed coherently with a signal field on a detector. The local oscillator enhances the signal intensities up to a factor of 100, and δn and δk can be separated by controlling the phase difference ($\Delta\phi$) between the local oscillator and the signal. Moreover, it has a linear relationship between the signal intensity and δn (or δk). However, the experimental setup of the OHD-TG is more complicated and difficult. A primary difficulty is to keep the phase stability between the local oscillator and the probe beam. A new simple OHD-TG setting has been reported [13–16] using an optical diffractive element to achieve sufficient phase stability. Terazima [17,18] reported the much improved and simple setting of the OHD-TG by using a tilt angle controlled neutral density filter to control the relative $\Delta\phi$ by changing the light path length. Katayama et al. [19–21] developed a

* Corresponding author. Fax: +1 626 683 9547.
E-mail address: kokamoto@caltech.edu (K. Okamoto).

0009-2614/$ - see front matter © 2005 Elsevier B.V. All rights reserved.
doi:10.1016/j.cplett.2005.08.020

lens-free OHD-TG technique by using a transmission grating structure in a 3 mm glass.

Recently, we have reported [22] the mask pattern transferred transient grating (MPT-TG) technique, which is a convenient new technique of the OHD-TG class with a metal film grating fabricated in our laboratory. We also showed that this technique is well applicable for highly sensitive molecular detection for micro fluidic devices [23]. In this Letter, this technique is applied to study the chemical reaction and molecular dynamics of photochromic molecule (spiropyran) in 2-propanol solution.

2. Method

Fig. 1a shows the pump and probe beams alignments for typical OHD-TG technique. Two pump beams (intensity: I_e, wavelength: λ_e) are crossed with angle (θ_e) to make optical interference pattern (optical grating, δI) at the sample. The fringe spacing (Λ) of the optical grating is given by $\Lambda = \lambda_e/2\sin\theta_e$. After that, δn and δk of the solution are also modulated along the optical grating. Both modulated δn and δk behave as diffraction gratings and can be detected by the first order diffracted beam of the probe beam (intensity: I_p, wavelength: λ_p). In order to enhance the diffracted signal intensity (I_s), the signal is superimposed to the reference beam (I_r) which provides a local oscillation field. As shown in Fig. 1a, four laser beams (two pump beams, a probe beam, and a reference beam) must be tuned one by one in order to focus at the same spot in the sample. Two pump beams must be controlled by an optical delay to maintain coherence. Thus the optical alignment of this technique is very complicated and difficult. Moreover, probe beam and reference beam must be tuned to keep $\Delta\phi$ stable. These tunings are tedious and unstable.

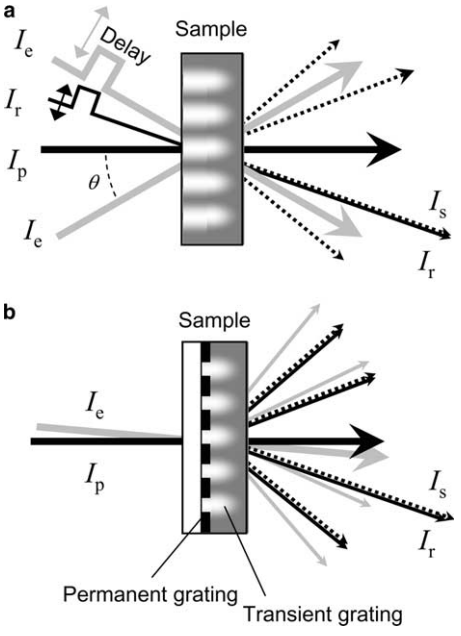

Fig. 1. Pump and probe beams alignments for (a) traditional optical heterodyne detected transient grating (OHD-TG) technique and (b) the present mask pattern transferred transient grating (MPT-TG) technique.

In contrast, Fig. 1b shows a schematic diagram of MPT-TG technique, which is both simple and stable by inserting a metal grating, eliminating one of the pump beams and the redundant I_r input. The tunings of delays or angles of these beams are not required, while it has the same advantage of the usual OHD-TG. The grating pattern is thus transferred from the metal film to the sample solution such that a similar optical grating is created. More details of the pattern transfer are shown in Fig. 2. At the bright region, many molecules are excited and chemical products are generated by this photochemical reaction. Therefore, molecular concentrations of chemical products are also spatially modulated (concentration grating, δC). Temperature in solution is also spatially modulated (thermal grating, δT) by the energy released though nonradiative relaxation from the excited molecules. Both δC and δT contribute to induced δn and δk. Further simplicity of this optical setting is that two types of the diffracted patterns are generated from the probe beams, namely diffraction from the metal grating and that from the transient grating. The former is an invariant diffracted light whereas the latter is variable since all δC, δT, δn, and δk are functions with time (t) and space (x). The invariant beam acts as a reference beam (I_r) to provide a local oscillation field and enhances the variable signal beam (I_s) by orders of magnitude. The conditions required for heterodyne detection are automatically satisfied, since both beams have completely the same originality, position and direction. In this setup, $\Delta\phi$ is decided only by the thickness of the metal grating. Therefore, the phase stability of this setup is excellent contrasted to the tuning difficulty and the unstable $\Delta\phi$ that characterize the usual OHD-TG.

3. Experimental

The experimental setup of the MGT-TG has already been published elsewhere [22,23]. A frequency-tripled Nd:YAG laser ($\lambda_e = 366$ nm, $I_e = 0.3$ mJ/pulse) and a cw-He–Ne laser ($\lambda_p = 633$ nm, $I_p = 0.05$ mW) are used as the pump and the probe beams, respectively. The pulse width and repetition rate of pump beam are 10 ns and 10 Hz, respectively. Both pump and probe beams are focused by a lens on the sample solution. The pump beam is not tightly focused (spot size $\sim$ 1 mm) on the sample to avoid any multiphoton process, higher

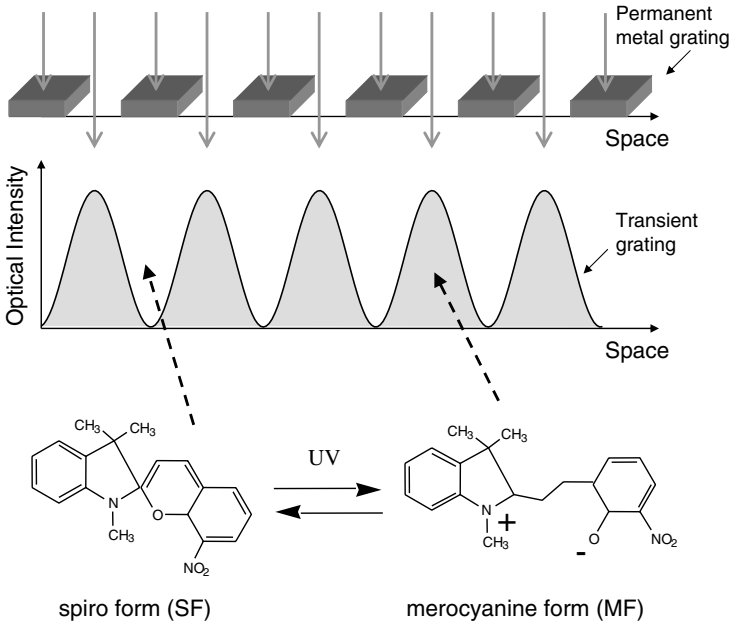

Fig. 2. Schematic diagram of the permanent metal grating and induced spatial modulation of light intensity. Spiropyran molecules were photoexcited and transformed from merocyanine form (MF) to spiro form (SP) along the bright–dark pattern.

order reaction, or transient lens contribution [17,18]. Two types of diffracted signal I_r and I_s are isolated from pump beam with a pinhole and a glass filter and detected with a InGaAs photodetector. Time profiles of the signals were measured with a 100 Hz digital oscilloscope.

To make a metal grating, chromium layer (100 nm) was deposited by the vacuum evaporation on the quartz substrate. A fine grade photo resist was deposited on a Cr layer by spin coating. Micrometer-scaled pattern are written by the lithography of a direct writing laser. Finally, metal grating structures are engraved by chemical etching. The grating period is $\Lambda = 9$ μm.

Sample solution used is spiropyran [1′,3′,3′-trimethyl-8-nitrospiro (2H-1-benzopyran-2,2′-indoline)] in 2-propanol. The concentration is about 5 mM. Photochemical reaction scheme of this molecule is shown in the bottom row of Fig. 2. The excited molecules produce colored isomer (merocyanine form; MF) while the ground state (spiro form, SF) is transparent at the probe wavelength. That is the reason why this molecule is called photochomic molecule. The spiropyran (Eastman Kodak) was purified by recrystallization. Spectroscopic grade solvent 2-propanol is used as received.

4. Results and discussion

Fig. 3 showed the time profiles of the TG signals in microsecond time scale (a) and millisecond timescale (b). The dashed line in each figure is the signal intensity of the reference beam (I_r). After excitation, the diffracted beam intensity rose rapidly and decayed with

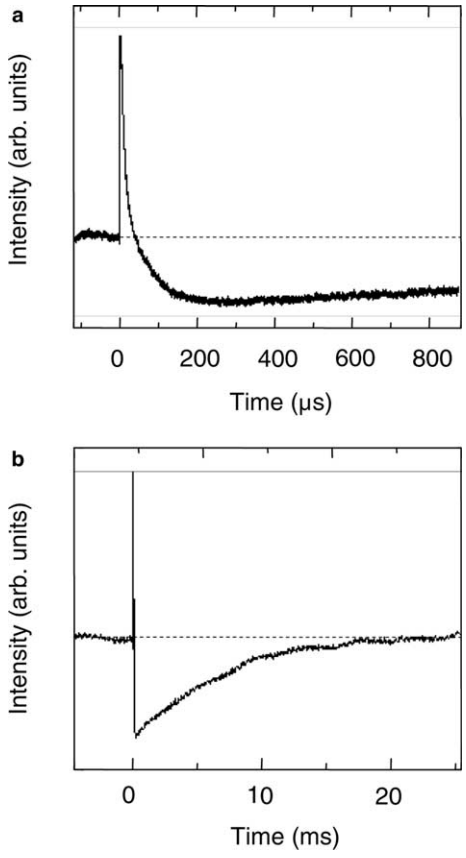

Fig. 3. Time profiles of the diffracted signals (TG signals) in microsecond timescale (a) and millisecond timescale (b). The dashed lines denote the initial intensities of the reference beam (I_r).

microsecond timescale. The signal decayed lower than base line ($t = 0$). This negative signal component decays with millisecond timescale and tends to the baseline finally. The total signal intensity (I_{total}) is given by [12,15–19]

$$I_{\text{total}}(t) = I_{\text{r}} + 2a[\chi^{(3)\prime}(t)\cos\Delta\phi + \chi^{(3)\prime\prime}(t) \times \sin\Delta\phi]I_{\text{e}}I_{\text{p}} + |\chi^{(3)}(t)|^2 I_{\text{e}}^2 I_{\text{p}}, \quad (1)$$

where $\chi^{(3)\prime}(t)$ and $\chi^{(3)\prime\prime}(t)$ are the real part and imaginary parts respectively of the third order nonlinear electrical susceptibility $\chi^{(3)}(t)$, and a is a real constant. The third term indicates the TG signal with usual homodyne detection and is negligible because $\chi^{(3)}$ in solution should be very small. Thus, only the second term of Eq. (1) indicates I_{s}, and this provides a large enhancement of the signal intensity and a linear relationship between the output signal and $\chi^{(3)}$. Obtained time-variable signal is the TG signal ($I_{\text{TG}}(t)$) corresponding to the second term of Eq. (1). In this case, $\chi^{(3)\prime}(t)$ and $\chi^{(3)\prime\prime}(t)$ are equal to $\delta n(t)$ and $\delta k(t)$ induced by the transient grating, respectively. Thus, the second term of Eq. (1) can be written by

$$I_{\text{TG}}(t) \cong \delta n(t)\cos\Delta\phi + \Delta\delta k(t)\sin\Delta\phi. \quad (2)$$

The origin of the fast decayed positive signal and the slow decayed negative signal observed in Fig. 3 should be different. As mentioned above, thermal grating (δT) and concentration grating (δC) can contribute to the signal time-profile. These contributions are given by the following relationships [9],

$$\delta n = \left[\left(\frac{\partial n}{\partial \rho}\right)_T \frac{\partial \rho}{\partial T} + \left(\frac{\partial n}{\partial T}\right)_\rho\right]\delta T + \left[\left(\frac{\partial n}{\partial \rho}\right)_C \frac{\partial \rho}{\partial C} + \left(\frac{\partial n}{\partial C}\right)_\rho\right]\delta C, \quad (3a)$$

$$\delta k = \left[\left(\frac{\partial k}{\partial \rho}\right)_T \frac{\partial \rho}{\partial T} + \left(\frac{\partial k}{\partial T}\right)_\rho\right]\delta T + \left[\left(\frac{\partial k}{\partial \rho}\right)_C \frac{\partial \rho}{\partial C} + \left(\frac{\partial k}{\partial C}\right)_\rho\right]\delta C, \quad (3b)$$

where ρ is density of the solution. Since both Eqs. (3a) and (3b) are linear, the relationship between $I_{\text{TG}}(t)$ and δT, δC should be also linear. By solving diffusion rate equations, the space and time behavior of both $\delta T(x,t)$ and $\delta C(x,t)$ can be obtained as exponential functions. Therefore, the following relationship is obtained:

$$I_{\text{TG}}(t) = \alpha T_0 \exp(-D_{\text{T}}q^2 t) + \beta C_0 \exp(-D_{\text{C}}q^2 t), \quad (4)$$

where D_{T} and D_{C} are the thermal diffusion coefficient of solution and concentration diffusion coefficient of solute molecule, respectively, α and β are constants. T_0 and C_0 are the initial values of the raised temperature and excited molecular concentration just after excitation ($t = 0$). q is the grating constant described by the grating period (Λ) as $q = 2\pi/\Lambda$. Thus, time-profiles of the TG signals are predictable from this equation. Usually thermal diffusion processes are much faster than concentration diffusion processes ($D_{\text{T}} \gg D_{\text{C}}$) in solutions. Therefore, the fast and slow decay components in Fig. 3 should be attributed to the thermal and concentration gratings components, respectively. It explains why observed thermal grating signal has positive sign whereas, the concentration grating signal has negative sign.

In this case, thermal grating only contributes to δn, and $(\partial n/\partial T)_\rho$ term in Eq. (3a) is negligible. Also, $(\partial n/\partial \rho)_{\text{T}}(\partial \rho/\partial T) < 0$ should be satisfied because solution densities generally decrease with increasing of temperature. Thus, $\delta n(t)$ in Eq. (2) should have negative sign when observed thermal signal has positive sign. This suggest that $\cos(\Delta\phi) < 0$ in Eq. (2). On the other hand, the concentration grating in this solution mainly contributes to δk because MF has large absorbance at the probe wavelength (633 nm). In contrast, the contribution of SF is negligible because the absorption band of SF is located at UV wavelength region. This fact has been reported using homodyne [24,25] and heterodyne [18] detected TG technique. Since molecular absorbance has positive sign, $\delta C(t)$ in Eq. (2) should have positive sign while observed thermal signal has negative sign. This suggest that $\sin(\Delta\phi) < 0$. Therefore, it is concluded that $180° < \Delta\phi < 270°$. The metal grating provides a permanent amplitude grating, which has 180° phase difference to the transient amplitude grating. The low absorbance regions of the metal grating (window) correspond to the high absorbance regions of the transient grating, because MF molecules were generated at these regions by the photochemical excitation. The other phase shift should be due to the optical pass length difference provided by the 100 nm thick metal grating film. This phase shift ranges between 0° and 90°, which seems reasonable because metal film thickness (100 nm) is smaller than 1/4 of the probe wavelength (633 nm). By changing the metal film thickness, $\delta n(t)$ or $\delta k(t)$ can be clearly separated with $\Delta\phi = 0°$, 180° or 90°, 270°, respectively. The controlling of $\Delta\phi$ is also available by the previous techniques [13–21], however, $\Delta\phi$ was very unstable. By using our technique, $\Delta\phi$ is almost permanently stable and still easy to control.

Since the decay time-scale of δT and δC are so different, each decay profile can be fitted by a single exponential function. Fig. 4 depicts the semi-log plot of the corresponding time-profiles of $\delta T(t)$ and $\delta C(t)$. Each profile shows a good exponential decay and the straight lines are fitted lines. By each signal decay rate, D_{T} and D_{C} are obtained as $D_{\text{T}} = 7.1 \pm 0.5 \times 10^{-8}\ \text{m}^2\ \text{s}^{-1}$ and $D_{\text{C}} = 3.0 \pm 0.2 \times 10^{-10}\ \text{m}^2\ \text{s}^{-1}$. D_{T} can be calculated by the thermal conductivity (κ), heat capacity (C_{p}), and ρ as $D_{\text{T}} = \kappa/\rho C_{\text{p}}$. The calculated value of D_{T} of

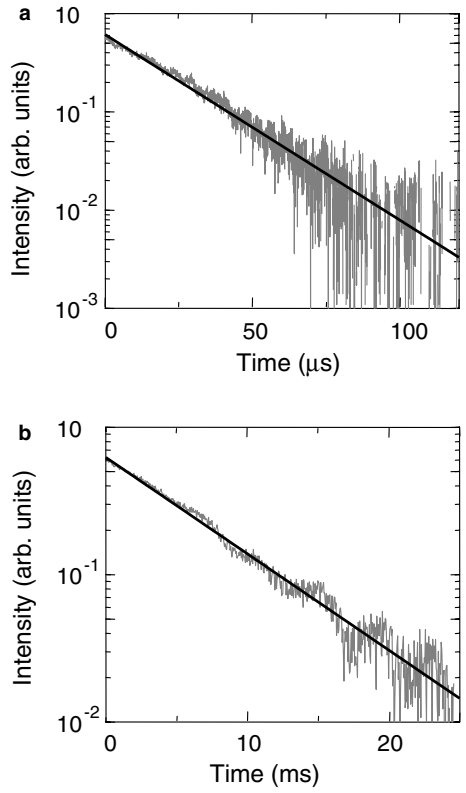

Fig. 4. Semi-log plots of the TG signals in microsecond timescale (a) and in millisecond timescale (b). The straight lines are best fits.

2-propanol is $D_T = 6.8 \times 10^8\ m^2\ s^{-1}$. The experimentally obtained D_T value is very close to the calculated value. D_C of MF in 2-propanol was previously obtained by the homodyne TG technique as $D_C = 2.7 \times 10^{-10}\ m^2\ s^{-1}$ [25]. This value also agrees with D_C obtained by MPT-TG here. Theoretically, concentration diffusion coefficients are given by the following Stokes–Einstein equation with solute molecular radius (r), solvent viscosity (η), Boltzmann constant (k_B), and T.

$$D_{SE} = \frac{k_B T}{a\eta r}, \tag{5}$$

where a is the constant which denote a boundary condition between solute and solvent. This depend on the molecular size/shape, solvent structure, and solute-solvent interaction, etc. and usually ranges between 4π (slip boundary) and 6π (stick boundary). The calculated D_{SE} values with slip and stick condition are $3.8 \times 10^{-10}\ m^2\ s^{-1}$ and $2.5 \times 10^{-10}\ m^2\ s^{-1}$, respectively. The obtained D_C value by MPT-TG is rather close to D_{SE} with stick condition. This fact has been already reported elsewhere [18,24]. The MF of spiropyran has large dipole moment due to the intramolecular charge separated feature as shown in Fig. 2. This property causes a strong intermolecular interaction with polar solution molecules such as 2-propanol [25]. Such strong interaction would bring a stick boundary condition between solute and solvent. Accordingly, we concluded that both the obtained D_T and D_C values are reasonable.

5. Conclusion

We used the MPT-TG technique for spiropyran in 2-propanol solution to observe the chemical reaction and molecular dynamics. We measured D_T and D_C values by the time-profile of the TG signal. Both observed values are in good agreement with the calculated value or and previous reported value. The MPT-TG technique has the same advantage to the usual OHD-TG techniques such as high sensitivity, well analyzable, and linear relationship of signal intensity vs. $\chi^{(3)}$. Moreover, this technique's merits also include a very simple setting, easy alignment, and excellent phase stability. Also $\Delta\phi$ should be controlled accurately by changing the metal grating thickness. The MPT-TG technique is expected to find broad applications in physics, chemistry, material, and biological study.

Acknowledgments

The authors thank Prof. M. Terazima (Kyoto University) for valuable suggestions and discussions. A part of this study was supported by the DARPA Center for Opto-fluidics, under Grant No. HR0011-04-1-0032.

References

[1] H.J. Eichler, P. Gunter, D.W. Pohl, Laser-induced Dynamic Grating, Springer, Berlin, 1986.
[2] K.A. Nelson, M.D. Fayer, J. Phys. Chem 72 (1980) 5202.
[3] L. Genberg, Q. Bao, S. Gracewaski, R.J.D. Miller, Chem. Phys. 131 (1989) 81.
[4] M. Terazima, K. Okamoto, N. Hirota, J. Phys. Chem 97 (1993) 5188.
[5] L. Dhar, J.A. Rogers, K.A. Nelson, Chem. Rev. 94 (1994) 157.
[6] J.A. Rogers, K.A. Nelson, J. Appl. Phys. 75 (1994) 1534.
[7] K. Okamoto, M. Terazima, N. Hirota, J. Chem. Phys. 103 (1995) 10445.
[8] K. Okamoto, N. Hirota, M. Terazima, J. Phys. Chem. A. 101 (1997) 5269.
[9] M. Terazima, Res. Chem. Intermed. 23 (1997) 853.
[10] K. Okamoto, N. Hirota, M. Terazima, T. Tominaga, J. Phys. Chem. A. 105 (2001) 6586.
[11] P. Vöhringer, N.F. Scherer, J. Phys. Chem. 99 (1995) 2684.
[12] W. Kohler, P. Rossmanith, J. Phys. Chem. 99 (1995) 5838.
[13] J.A. Rogers, M. Fuchs, M.J. Banet, J.B. Hanselman, R. Logan, K.A. Nelson, Appl. Phys. Lett. 71 (1997) 225.
[14] A.A. Maznev, K.A. Nelson, J.A. Rogers, Opt. Lett. 23 (1998) 1319.
[15] G.D. Goodno, G. Dadusc, R.J.D. Miller, J. Opt. Soc. Am. B 15 (1998) 1791.
[16] Q.-H. Xu, Y.-Z. Ma, G.R. Fleming, Chem. Phys. Lett. 338 (2001) 254.
[17] M. Terazima, Chem. Phys. Lett. 304 (1999) 343.

[18] M. Terazima, J. Phys. Chem. A 103 (1999) 7401.
[19] K. Katayama, M. Yamaguchi, T. Sawada, Appl. Phys. Lett. 82 (2003) 2775.
[20] M. Yamaguchi, K. Katayama, T. Sawada, Chem. Phys. Lett. 377 (2003) 589.
[21] K. Katayama, M. Yamaguchi, T. Sawada, J. Appl. Phys. 94 (2003) 4904.
[22] K. Okamoto, Z. Zhang, A. Scherer, D.T. Wei, Appl. Phys. Lett. 85 (2004) 4842.
[23] K. Okamoto, Z. Zhang, D.T. Wei, A. Scherer, Thin Solid Films 469–470 (2004) 420.
[24] T. Okazaki, N. Hirota, M. Terazima, J. Photochem. Photobiol. 99 (1996) 155.
[25] K. Okamoto, N. Hirota, M. Terazima, to be published.